

# High-speed growth and photoluminescence of porous anodic alumina films with controllable interpore distances over a large range

Y. B. Li and M. J. Zheng<sup>a)</sup>

Laboratory of Condensed Matter Spectroscopy and Opto-Electronic Physics, Department of Physics, Shanghai Jiao Tong University, Shanghai 200240, People's Republic of China

L. Ma

School of Chemistry and Chemical Technology, Shanghai Jiao Tong University, Shanghai 200240, People's Republic of China

(Received 25 June 2007; accepted 25 July 2007; published online 16 August 2007)

Highly ordered porous anodic alumina (PAA) films are fabricated with high efficiency by stable high-field anodization in oxalic acid/ethanol/water electrolytes at 100–180 V and sulfuric acid/oxalic acid/ethanol/water electrolytes at 30–80 V, giving interpore distances in the range of 225–450 nm and 70–140 nm, respectively. The photoluminescence of PAA films prepared by high-field anodization shows remarkable redshift of the peak position and decrease of the intensity compared to that of PAA films formed by conventional low-field anodization. © 2007 American Institute of Physics. [DOI: 10.1063/1.2772184]

In recent years, porous anodic alumina (PAA) films have been extensively used as templates, mask, or host materials to synthesize various nanostructures in the forms of nanopores,<sup>1,2</sup> nanowires,<sup>3</sup> nanotubes,<sup>4</sup> and nanodots,<sup>5</sup> which could be used as building blocks for developing nanoscale devices.

The conventional two-step anodization process<sup>1,6,7</sup> produces PAA films with limited ordered domain sizes, and the interpore distances of the films are confined to several fixed values. The pretexturing techniques<sup>8–13</sup> can produce PAA films with very large ordered domain sizes and provide flexibility in controlling interpore distances, but these techniques require sophisticated and expensive pretreatment processes. Moreover, in both cases, long anodizing time is required to obtain relatively high aspect ratios due to very low anodizing current densities and hence very slow film-growth rates. The high-field anodization process<sup>14–17</sup> not only produces highly ordered PAA films with very high efficiency, but also expands the regime of self-ordering that is unexplored by conventional two-step anodization process, thus has provoked considerable research interest over the past three years.

Recently, we employed ethanol as a coolant for the electrolysis, which have been proven to be quite effective and simple for realizing stable high-field anodization in  $\text{H}_3\text{PO}_4\text{-C}_2\text{H}_5\text{OH-H}_2\text{O}$  electrolytes.<sup>17</sup> In this letter, we further demonstrate that our approach can be applied to sulfuric acid and oxalic acid electrolytes. The photoluminescence (PL) spectra of the PAA films formed by high-field anodization show a remarkable difference from that of PAA films formed under low-field conditions.

The fabrication processes used here were similar to that in  $\text{H}_3\text{PO}_4\text{-C}_2\text{H}_5\text{OH-H}_2\text{O}$  electrolytes.<sup>17</sup> Round aluminum foils (99.999% purity) with a radius of 1 cm were degreased in acetone, washed in de-ionized water, and put into a tailor-made holder with an opening of 2 cm<sup>2</sup>. Before anodizing, the aluminum was electropolished at a constant voltage in a 1:4 volume mixture of perchloric acid and ethanol under room temperature. The  $\text{C}_2\text{H}_2\text{O}_4\text{-C}_2\text{H}_5\text{OH-H}_2\text{O}$  electrolytes,

$\text{H}_2\text{SO}_4\text{-C}_2\text{H}_2\text{O}_4\text{-C}_2\text{H}_5\text{OH-H}_2\text{O}$  electrolytes, and  $\text{H}_2\text{SO}_4\text{-C}_2\text{H}_5\text{OH-H}_2\text{O}$  electrolytes are designated as S1, S2, and S3, respectively. For anodizations in S1, the concentrations of oxalic acid in the electrolytes were in the range of 0.1–0.5M, the temperatures of the electrolytes were kept at –10–0 °C, samples were anodized at target voltages (100–180 V) for 10 min. For anodizations in S2, the concentrations of sulfuric acid were in the range of 0.05–0.5M and the concentrations of oxalic acid in the electrolytes were fixed to 0.5M, the temperatures of the electrolytes were kept at –5–0 °C, samples were anodized at target voltages (30–80 V) for 10 min. Moreover, for both electrolytes, a 1:4 volume mixture of ethanol (99.7% purity) and de-ionized water was used as the solvent. Anodizations were performed in these electrolytes with vigorous stirring in a large glass beaker (2 l), cooled by a powerful low-constant temperature bath. After removing the remained aluminum on the back side, pore opening was conducted in a 5 wt %  $\text{H}_3\text{PO}_4$  solution at 30–45 °C for 30 min. The morphology of the samples was observed using a field-emission scanning electron microscope (FESEM) (Philips Sirion 200). The room-temperature PL emission spectra of the PAA films were measured by a Jobin Yvon ultraviolet-visible monochromator under a 325 nm He–Cd laser excitation.

Figure 1 shows the FESEM images of self-ordered PAA films formed by high-field anodization in S1. Interpore distances ( $D_{\text{int}}$ ) in the range of 225–450 nm were obtained. The interpore distance increases linearly with the anodizing voltage ( $E_a$ ) in the range of 100–160 V [Figs. 1(a)–1(g)]. The ratios of  $D_{\text{int}}$  (in nanometers) to  $E_a$  (in volts) are approximately 2.25 in this region. The interpore distance increases dramatically from 360 to 420 nm when the anodizing voltage changes from 160 to 170 V. The ratios of  $D_{\text{int}}$  to  $E_a$  for PAA films formed under 170 and 180 V are about 2.5 [Figs. 1(h) and 1(i)]. As proven in our previous work,<sup>17</sup> the ratio of  $D_{\text{int}}$  to  $E_a$  is exponentially decreased with the increase of anodizing current density ( $i_a$ ). As in the case of Lee *et al.*,<sup>16</sup> the anodizing current densities also decreased exponentially with the anodizing time in our case. The current density decreased rapidly for the first 2 min, falling to a level about 1/3 of the initial current density. Then, it decreased more

<sup>a)</sup> Author to whom correspondence should be addressed; electronic mail: mjzheng@sjtu.edu.cn

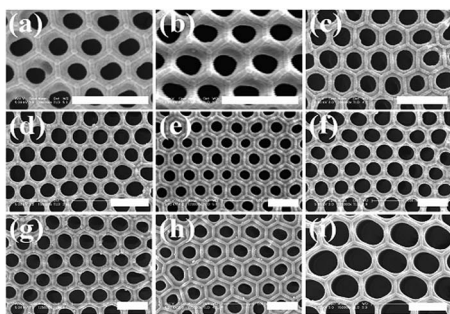


FIG. 1. FESEM bottom view of self-ordered PAA films formed by high-field anodization in S1 at 100–180 V,  $-10-0^{\circ}\text{C}$  for 10 min: (a) 100 V,  $D_{\text{int}} \approx 225$  nm; (b) 110 V,  $D_{\text{int}} \approx 250$  nm; (c) 120 V,  $D_{\text{int}} \approx 270$  nm; (d) 130 V,  $D_{\text{int}} \approx 290$  nm; (e) 140 V,  $D_{\text{int}} \approx 315$  nm; (f) 150 V,  $D_{\text{int}} \approx 340$  nm; (g) 160 V,  $D_{\text{int}} \approx 360$  nm; (h) 170 V,  $D_{\text{int}} \approx 420$  nm; and (i) 180 V,  $D_{\text{int}} \approx 450$  nm. The length of the inserted scale bars is 500 nm.

gradually for the rest of the anodization. Since the interpore distances were measured from the bottom side of the PAA films, the current densities at the end of the anodization should be considered. For anodizations under 100–160 V, the anodizing current densities fell from 3000–4000 to about  $300\text{ A m}^{-2}$ ; for anodizations under 170–180 V, the anodizing current densities fell from 2000–3000 to about  $50\text{ A m}^{-2}$ . This is why the ratios of  $D_{\text{int}}$  to  $E_a$  for PAA films formed under 170 and 180 V are larger than those formed under 100–160 V. Since the lower current densities will lead to lower extent of the order of pore arrangement, this also explains the decrease of extent of the ordering for PAA films formed under 170 and 180 V. The above experimental findings suggest that the current density should be maintained at a certain level to achieve highly ordered PAA films with a desired interpore distance at a given anodizing voltage.

The appearance of the PAA films formed in S1 under high fields (100–180 V) exhibited a golden color with high film toughness. The thickness of the PAA films formed by high-field anodization in S1 for 10 min is about  $20-30\text{ }\mu\text{m}$ . Because the growth rate of the oxide film is proportional to the anodizing current density, the exponential decrease of the anodizing current density results in uneven film-growth rate during the anodization. It decreases quickly with anodizing time as the anodizing current density falls. In order to have a high film-growth rate, the anodizing current density should be maintained at a high level for a given anodizing voltage. Thus, it can be seen that the main problem of high-field anodization in oxalic acid solutions is the exponential decrease of the anodizing current density, which should be addressed in future studies.

Figure 2 exhibits the FESEM images of highly ordered PAA films formed by high-field anodization in S2. The interpore distances of the PAA films are in the range of 70–140 nm. For high-field anodization in S1 at the voltages below 100 V, ordered pore arrangement cannot be achieved. Thus, we first tried to fabricate PAA films at the voltages below 100 V in S3. However, we found that although PAA films formed by high-field anodization in S3 have very good pore arrangements, the appearance of the films was very poor and the films were very fragile. To facilitate their practical applications, PAA films with good pore arrangements and mechanical properties are both required. Since PAA films formed in S1 have very good film toughness and appearance, we expected that PAA films with good pore arrangements and favorable mechanical properties could be obtained by

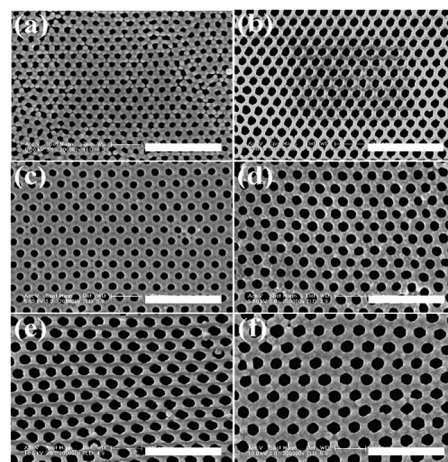


FIG. 2. FESEM bottom view of highly ordered PAA films fabricated by high-field anodization in S2 at 30–80 V,  $-5-0^{\circ}\text{C}$  for 10 min: (a) 30 V,  $D_{\text{int}} \approx 70$  nm; (b) 40 V,  $D_{\text{int}} \approx 80$  nm; (c) 50 V,  $D_{\text{int}} \approx 90$  nm; (d) 60 V,  $D_{\text{int}} \approx 105$  nm; (e) 70 V,  $D_{\text{int}} \approx 120$  nm; and (f) 80 V,  $D_{\text{int}} \approx 140$  nm. The length of the inserted scale bars is 500 nm.

high-field anodization in electrolytes containing both  $\text{H}_2\text{SO}_4$  and  $\text{C}_2\text{H}_2\text{O}_4$ . The experimental results proved our expectation: the appearance and toughness of the PAA films formed by high-field anodization in S2 were greatly improved compared with those formed in S3; and the pore arrangement of PAA films formed in S2 at 30–80 V is highly regular over a large area, as shown in Fig. 2. The ordering of the pore arrangement is almost insensitive to the anodizing voltage because the anodizing current densities were all maintained at a high level ( $>1000\text{ A m}^{-2}$ ). The anodizing current densities also decreased during the anodization, but the extent was smaller compared with what happened for anodization in S1. The anodizing current densities decreased from about 5000 to 1000–3000  $\text{A m}^{-2}$ . This further proves the importance of high anodizing current density in the formation of highly ordered PAA films. Higher anodizing current densities also led to faster film growth: the thickness of PAA films formed by high field (30–80 V) in S2 for 10 min was about  $40-80\text{ }\mu\text{m}$ .

Figure 3 gives the summary of self-ordering voltages and corresponding interpore distances in high-field anodization in three types of electrolyte used in our experiments. It shows that the regime of self-ordering achieved by our ap-

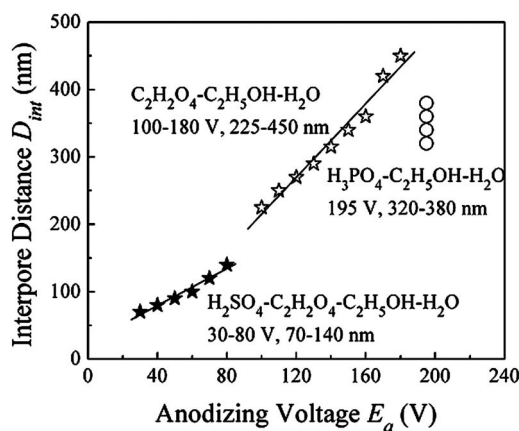


FIG. 3. Regime of self-ordering for high-field anodization in S1 (open stars), S2 (filled stars), and  $\text{H}_3\text{PO}_4-\text{C}_2\text{H}_5\text{OH}-\text{H}_2\text{O}$  electrolytes (open circles).

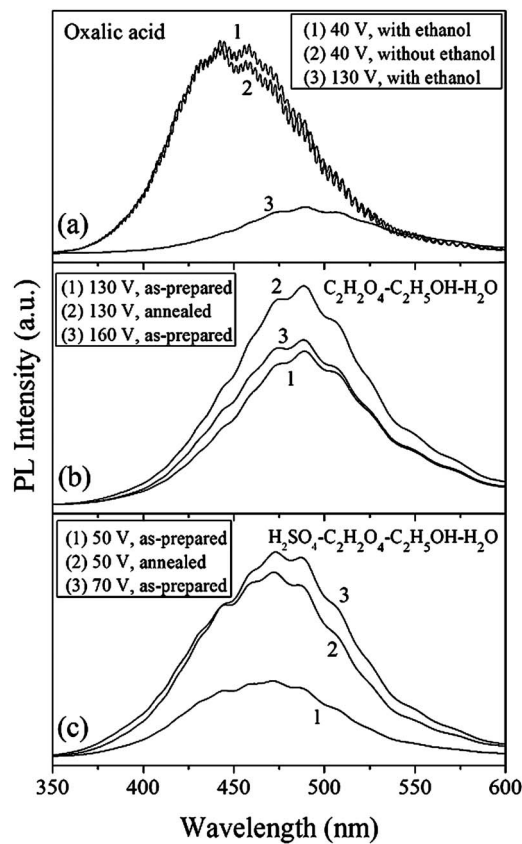


FIG. 4. Room-temperature PL spectra of the PAA films formed under different anodizing conditions, using a 325 nm laser as excitation.

proach covers almost the entire regime from 70 to 450 nm. This indicates that our approach is quite effective for it is possible to obtain any  $D_{\text{int}}$  in this range under proper anodizing conditions. Since the pores of the PAA films can be readily widened by chemical etching, the fabrication of highly ordered PAA films with any desired  $D_{\text{int}}$  in a wide range is the most important for their applications.

Figure 4 shows the room-temperature PL spectra of the PAA films formed under different anodizing conditions. Curves 1 and 2 in Fig. 4(a) show the PL spectra of PAA films ( $\sim 20 \mu\text{m}$  thickness) formed at 40 V for 10 h, with and without ethanol. The oscillations in the PL spectra are ascribed to the interference within a Fabry-Pérot optical cavity.<sup>18</sup> The two PL spectra are almost the same, which indicate that the ethanol in the electrolyte has little influence on the PL property of the PAA films. Curve 3 in Fig. 4(a) shows the PL spectrum of the PAA film ( $\sim 20 \mu\text{m}$  thickness) formed at 130 V. Compared with the PL spectrum of PAA film formed at 40 V, the PL peak shifts from  $\sim 440$  to  $\sim 490$  nm and the intensity is much smaller. For PAA films formed in oxalic acid, two PL bands were usually observed, which were centered at  $\sim 400$  and  $\sim 470$  nm, corresponding to the luminescence structures of  $\text{F}^+$  centers (singly ionized oxygen vacancies) and transformed carboxylic impurities, respectively.<sup>19–21</sup> This indicates that the redshift of the peak position and decrease of the PL intensity should be due to the decrease of singly ionized oxygen vacancies in PAA films under high-field conditions. The transformed carboxylic impurities were predominant in the PL band of PAA films formed under high-field conditions. Figures 4(b) and 4(c) show the PL spectra of PAA films formed at different high-

field conditions. It can be seen that the PL intensity is higher in the sample formed under higher anodizing voltage in the same electrolyte system. Moreover, the PL intensity increased after annealing the sample at 400 °C for 1 h. This implies that more oxalic impurities were transformed into luminescent centers by higher electric field or by Joule heating.<sup>21</sup>

In conclusion, we have demonstrated that by employing ethanol as coolant, stable high-field anodization can be realized in  $\text{C}_2\text{H}_2\text{O}_4\text{-C}_2\text{H}_5\text{OH-H}_2\text{O}$  and  $\text{H}_2\text{SO}_4\text{-C}_2\text{H}_2\text{O}_4\text{-C}_2\text{H}_5\text{OH-H}_2\text{O}$  electrolytes, resulting in highly ordered PAA films with  $D_{\text{int}}$  in the range of 225–450 nm and 70–140 nm, respectively. The highly ordered PAA films with controllable interpore distances in a large range could be used as templates to synthesize various nanostructures, which are important for developing nanodevices. The PL spectra of PAA films prepared under different conditions show that there are less singly ionized oxygen vacancies and the transformed carboxylic impurities dominate the PL band for PAA films formed by high-field anodization. The study of PL properties of the PAA films formed by high-field anodization is of technological importance from the viewpoints of both the PAA films and the synthesized nanomaterials.

This work was supported by the Natural Science Foundation of China of 50572064 and National Minister of Education Program for Changjiang Scholars and Innovative Research Team in University (PCSIRT).

<sup>1</sup>H. Masuda and K. Fukuda, *Science* **268**, 1466 (1995).

<sup>2</sup>G. Q. Ding, W. Z. Shen, M. J. Zheng, and D. H. Fan, *Appl. Phys. Lett.* **88**, 103106 (2006).

<sup>3</sup>G. Sauer, G. Brehm, S. Schneider, K. Nielsch, R. B. Wehrspohn, J. Choi, H. Hofmeister, and U. Gösele, *J. Appl. Phys.* **91**, 3243 (2002).

<sup>4</sup>G. Che, B. B. Lakshmi, E. R. Fisher, and C. R. Martin, *Nature (London)* **393**, 346 (1998).

<sup>5</sup>H. Masuda, K. Yasui, and K. Nishio, *Adv. Mater. (Weinheim, Ger.)* **12**, 1031 (2000).

<sup>6</sup>H. Masuda, F. Hasegawa, and S. Ono, *J. Electrochem. Soc.* **144**, L127 (1997).

<sup>7</sup>H. Masuda, K. Yada, and A. Osaka, *Jpn. J. Appl. Phys., Part 2* **37**, L1340 (1998).

<sup>8</sup>H. Masuda, H. Yamada, M. Satoh, H. Asoh, M. Nakao, and T. Tamamura, *Appl. Phys. Lett.* **71**, 2770 (1997).

<sup>9</sup>I. Mirkulskas, S. Juodkazis, R. Tomasianas, and J. G. Dumas, *Adv. Mater. (Weinheim, Ger.)* **13**, 1574 (2001).

<sup>10</sup>J. Choi, Y. Luo, R. B. Wehrspohn, R. Hillebrand, J. Schilling, and U. Gösele, *J. Appl. Phys.* **94**, 4757 (2003).

<sup>11</sup>N. W. Liu, A. Datta, C. Y. Liu, and Y. L. Wang, *Appl. Phys. Lett.* **82**, 1281 (2003).

<sup>12</sup>S. Fournier-Bidoz, V. Kitaev, D. Routkevitch, I. Manners, and G. A. Ozin, *Adv. Mater. (Weinheim, Ger.)* **16**, 2193 (2004).

<sup>13</sup>H. Masuda, Y. Matsui, M. Yotsuya, F. Matsumoto, and K. Nishioy, *Chem. Lett.* **33**, 584 (2004).

<sup>14</sup>S. Ono, M. Saito, and H. Asoh, *Electrochem. Solid-State Lett.* **7**, B21 (2004).

<sup>15</sup>S. Z. Chu, K. Wada, S. Inoue, M. Isogai, and A. Yasumori, *Adv. Mater. (Weinheim, Ger.)* **17**, 2115 (2006).

<sup>16</sup>W. Lee, R. Ji, U. Gösele, and K. Nielsch, *Nat. Mater.* **5**, 741 (2006).

<sup>17</sup>Y. B. Li, M. J. Zheng, L. Ma, and W. Z. Shen, *Nanotechnology* **17**, 5101 (2006).

<sup>18</sup>K. Huang, L. Pu, Y. Shi, P. Han, R. Zhang, and Y. D. Zheng, *Appl. Phys. Lett.* **89**, 201118 (2006).

<sup>19</sup>W. L. Xu, M. J. Zheng, S. Wu, and W. Z. Shen, *Appl. Phys. Lett.* **85**, 4364 (2004).

<sup>20</sup>Y. Du, W. L. Cai, C. M. Mo, J. Chen, L. D. Zhang, and X. G. Zhu, *Appl. Phys. Lett.* **74**, 2951 (1999).

<sup>21</sup>Y. Yamamoto, N. Baba, and S. Tajima, *Nature (London)* **289**, 572 (1981).